



Poly(vinylidene fluoride) (PVDF) membrane fabrication with an ionic liquid via non-solvent thermally induced phase separation (N-TIPs)

Ting He^{1,2,3} · Xiaogang Li^{1,2,3} · Qian Wang^{1,2,3} · Yue Zhou^{1,2,3} · Xiaozu Wang^{1,2,3} · Zhaohui Wang^{1,2,3} · Naser Tavajohi⁴ · Zhaoliang Cui^{1,2,3}

Received: 2 February 2021 / Accepted: 16 September 2021 / Published online: 11 February 2022
© The Author(s) 2022

Abstract

In this paper, ionic liquid 1-butyl-3-methylimidazolium tetrafluoroborate was the first time successfully utilized as single solvent in preparing the PVDF membrane with a good performance by N-TIPs method. The effects of quenching temperature and hydrophilic additive content on the morphology, permeability, and strength of the membranes were studied. All the prepared PVDF membranes were proved to be a pure β phase by FTIR and XRD, possessing a narrow pore size distribution. By adjusting quenching temperature and additive content, membranes with a flux of 383.2 L/m² h and concentrated pore diameter of 26 nm obtained.

Keywords PVDF membrane · β phase · Ionic liquid · N-TIPS

Introduction

Membrane technology is called "the water treatment technology of the twenty-first century", which can be used to separate, grade, purify or enrich constituent systems. Polyvinylidene fluoride (PVDF) is formed by homopolymerization or copolymerization of vinylidene fluoride monomers. Due to the high binding energy of fluorocarbon chain, PVDF has excellent chemical corrosion resistance, high temperature color change resistance, oxidation resistance, ultraviolet resistance and high-energy radiation resistance. It also has strong wear resistance, flexibility, swelling strength, impact

resistance strength, and pollution resistance, making it an ideal raw material for ultrafiltration membranes.

PVDF can exist in five distinct crystalline phases, the β -phase possessing an all-trans (TTT) planar zigzag conformation (Kepler and Anderson 1978; Lovinger 1982; Salimi and Yousefi 2003). Each polymer chain in the β phase has a dipole moment oriented perpendicular to its long axis originating from the separation of the CF₂ and CH₂ groups. Consequently, β -phase PVDF has electroactive properties including piezo, pyro, and ferroelectricity, and thus therefore can be used in wide specific applications (Martins et al. 2014); it has been used in piezoelectric membranes separation (Lee et al. 2004; Ohigashi et al. 1991; Deha and Kumar 2011; Wormald et al. 2006; Martins et al. 2011; Imai et al. 2012; Ribeiro et al. 2012).

Coster et al. found that "poling" commercial α -phase dominant PVDF membranes in an intense AC electric field improved their flux by 136% on average (Coster et al. 2011). Su et al. reported that membranes with finger-like structures had higher dielectric strengths and also exhibited more piezoelectric properties, reducing the transmembrane pressure increase by 66% after poling these membranes (Su et al. 2021).

One of the current challenges in the membrane is sustainability in the membrane fabrication process. By increasing the environmental restrictions, membrane producers are facing numerous challenges to reduce the environmental impact

✉ Xiaozu Wang
wangxiao@163.com

✉ Zhaohui Wang
zhwang@njut.edu.cn

¹ State Key Laboratory of Materials-Oriented Chemical Engineering, College of Chemical Engineering, Nanjing Tech University, Nanjing 210009, China

² National Engineering Research Center for Special Separation Membrane, Nanjing Tech University, Nanjing 210009, China

³ Jiangsu National Synergetic Innovation Center for Advanced Materials (SICAM), Nanjing Tech University, Nanjing 210009, China

⁴ Department of Chemistry, Umeå University, 90187 Umeå, Sweden

of membrane production, including the use of toxic solvents. Membrane preparation often involves the use of very toxic solvents (Garcia-Ivars et al. 2014) which severely limit the ability to work under safe conditions for human health and for the environment. Considering the increasing awareness of the environmental impacts of chemical products, the use of solvents that are nonhazardous to human health and the environment will play a key role in sustainable membrane preparation in the near future.

The toxicity of the solvents and the urgent need for green solvents for membrane manufacturing was pointed out by Cui et al. (Cui et al. 2013; Hassankiadeh et al. 2015). This work was followed by introducing water-soluble green solvent (Cui et al. 2015a) and a water-soluble, biodegradable green solvent for membrane fabrication (Hassankiadeh et al. 2015). This research was complemented by other researchers during the past years and the concept of the green membrane was introduced by researchers to have sustainable membrane production (Szekely et al. 2014).

One interesting class of solvents for fabricating membrane is Ionic Liquids. Ionic liquid (IL) is non-polluting, odorless, recyclable, thermally and chemically stable, and can be easily separated from products. Different from other organic solvents, ILs is generally not entering into the steam due to its negligible vapor pressure, so the air pollution caused by harmful gases in chemical experiments can be avoided. It is an ideal substitute for traditional volatile solvent, which can alleviate the serious problems related to the environment, human health and safety, and equipment corrosion effectively.

Ionic liquid, 1-ethyl-3-methylimidazolium acetate was used as solvents to prepare cellulose acetate and polyacrylonitrile membranes by non-solvent-induced phase separation, respectively (Livazovic et al. 2015; Kim et al. 2016). In our previous study, we demonstrated ionic liquids potential to fabricate poly(ethylene chlorotrifluoroethylene) membrane by thermally induced phase inversion (Yue and Cheng 2018). In the present study, a new type of ionic liquids 1-butyl-3-methylimidazolium tetrafluoroborate is used as a solvent to demonstrate the potential of ionic liquids for fabricating membrane by a combination of non-solvent-induced phase inversion and thermally induced phase separation (N-TIPs). The potential of new solvent, the effect of membrane preparation parameters, and the performance of the fabricated membranes were investigated. Pure β -phase PVDF membranes with a narrow pore size distribution were successfully obtained.

Experimental

Materials

PVDF (Solef® 1015, powder, Mw = 40,000) was purchased from Solvay Industry (shanghai, China) Co. Ltd. [BMIM]

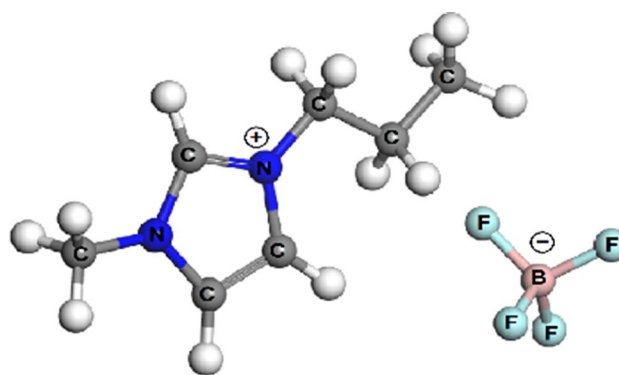


Fig. 1 Chemical structure of [BMIM]BF₄

Table 1 Properties of [BMIM]BF₄

Formula	C ₈ H ₁₅ N ₂ BF ₄
Molecular weight(g/mol)	226.02
Purity(%)	> 99.0
Specific gravity(g/cm ³)	1.26
Viscosity(cP)	140 (20 °C)
Decomposition temperature(°C)	403
Soluble in	Water, ethanol, acetonitrile
Insoluble in	Ethyl acetate, ethyl ether

BF₄ (see chemical structure in Fig. 1 and properties in Table 1) was purchased from Lanzhou Materialization Institute. Poly(vinylpyrrolidone) PVP k30 (Mw = 40,000) and ethanol were supplied by Sinopharm Chemical Reagent Co., Ltd (Shanghai, China). Deionized water was made by a home-made RO system. Kerosene was purchased from Aladdin Biochemical Technology Co., Ltd.

Phase diagram

The phase diagram is an important tool to analyze the thermodynamic aspect of phase inversion. It consists of the crystallization line and cloud point curve. A series of casting solutions were prepared using PVDF and IL as samples (polymer concentration was 10 wt%, 20 wt%, 30 wt%, 40 wt%, 50 wt%).

Crystallization line is measured by Differential Scan Calorimeter (DSC Q-20, TA Instruments, USA). A certain amount of PVDF/IL casting solution was weighed and transferred to the sample plate. The sample is then heated to 200 °C at the speed of 10 °C/min. It was maintained at this temperature for 5 min to eliminate the thermal history of the casting solution. The sample is then cooled to 20 °C at a rate of 10 °C/min, and the crystallization temperature is the peak temperature of the exothermic peak.

The cloud point curve is measured by Polarizing microscope (XPV-800E, BIMU, Shanghai, China). A small amount of sample is sandwiched between two slide glasses and placed on the hot table (KER3101-500S). The hot table is heated rapidly to 200 °C and maintained for 5 min to eliminate the heat history. The sample is then cooled to room temperature. The cloud point temperature was determined visually by observing the appearance of turbidity under the polarizing microscope.

Membrane fabrication

A certain amount of PVDF 1015 powder, [BMIM]BF₄ (liquid) and PVP K30 were weighed and added into a 100 mL silk bottle and were sealed prior to use. The solution was stirred in an oil bath with the temperature of 180 °C and a homogeneous solution was obtained. Then, the solution was settled in the oil bath for 2 h to de-gas. Afterward, the casting solution was cast in a high temperature scraper onto a glass plate, of which the temperature is the same as the casting solution. Then, the glass plate was immersed into water bath with different temperature to obtain the original flat sheet membrane. The original flat sheet membrane was immersed into deionized water for 12 h and then immersed into ethanol for 12 h to extract the diluent. This operation was repeated for three times.

Membrane characterization

The pure water flux of the flat sheet membrane was measured by a dead-end laboratory-made machine. First, the machine was operated under the pressure of 0.15 MPa for about 5 min. After the water permeate became stable, the pure water flux can be tested. It was measured under the pressure of 0.1 MPa, and the data was recorded every 3 min. The tests were repeated five times for the membranes that were prepared under the same conditions. The average value was defined as the pure water flux of the prepared PVDF membrane.

The pure water flux was calculated by the following formula:

$$J = \frac{V}{A \cdot t} \quad (1)$$

where J is the pure water flux (L/m² h), and V is the volume of the permeate water (L). A and t are the effective area of the tested membrane (m²) and the tested time (h), respectively.

The porosity was measured by the weigh method, of which the wetting medium is kerosene. First, the flat sheet membrane was taken out from the pure water and dried in a vacuum oven for 5 h under the temperature of 50 °C. Then, the weight of the dried membrane was weighted and

recorded. Afterward, the dried membrane was immersed in kerosene for 48 h and taken out. The kerosene on the surface of the membrane was wiped out and weighed on the balance, which was defined as the weight of the wetted membrane. The overall porosity of the membranes was calculated according to following correlation:

$$\varepsilon = \frac{(w_w - w_d)/\rho_k}{(w_w - w_d)/\rho_k + w_d/\rho_p} \times 100\% \quad (2)$$

where w_w is the weight of the wet membrane (g), and w_d is the weight of the dried membrane (g). ρ_k and ρ_p are the density of kerosene (0.82 g/cm³) and PVDF (1.78 g/cm³), respectively. ε is the porosity of the membrane (%).

X-ray diffractometry (XRD). To analyze the crystalline structure of the bulk PVDF membranes, an X-ray diffractometer (XRD) (D8 Advance, Bruker, Germany) was used with a scanning angle ranging from 10° to 30° and a scanning velocity of 1.6°/min at room temperature. The operating voltage and current were 40 kV and 30 mA, respectively, plasticine was used as a holder for samples, and Cu K_α radiation was applied.

To obtain accurate crystalline structural information of the top/bottom skin layers of the membrane as well as the area immediately beneath, an ATR-FTIR (Bio-Rad FTIR FTS 135) was used in attenuated total reflection (ATR) mode with a spectral range of 400–1500 cm⁻¹ under nitrogen purging. With a penetration depth of a few microns, ATR-FTIR can identify the characteristic ATR spectra of various functional groups in the skin layers of the flat sheet membranes, which is different from the results obtained from the XRD analysis on the crystalline structure of the bulk membranes.

To observe the fabricated membrane morphology the pre-dried PVDF membranes were immersed and broken in liquid nitrogen, After coated with palladium, field emission scanning electronic microscopy (FESEM, Hitachi S4800, Japan) was employed to observe the surfaces and cross sections of the prepared PVDF membranes.

The contact angle was measured by DropMeter A-100 (MAIST Measurement Co., Ltd., China). A 0.4 μL droplet of DI water was dropped onto the membrane surface at room temperature, and the image was captured by a digital camera, showing the apparent static contact angle. Each sample was measured at five different positions to obtain the average value.

The mean pore size and pore size distribution of PVDF membranes were measured by liquid replacement method. The liquid–liquid displacement porometry (LLDP) was purchased from Gao Qian Functional Materials Co., Ltd. Nanjing China. The volume ratio of isobutanol to pure water is 1:1. After full mixing and phase separation, the lower layer water is the infiltration liquid and the upper isobutanol is

the replacement liquid. The interfacial tension of the two immiscible phases was $1.7 \times 10^{-3} \text{ N}\cdot\text{m}^{-1}$. The relationship between the radius (r) of the membrane pores and the pressure (P) required to pass through the membrane pores is as follows (Cui et al. 2018a):

$$P = \frac{2\delta}{r} \cos \theta \quad (3)$$

where R (m) is the radius of the membrane pore; P (MPa) is the pressure required for gas to pass through the membrane pore; and θ ($^\circ$) is the contact angle between the wetting agent and the surface of the membrane. The surface tension of the wetting agent is δ ($1.7 \times 10^{-3} \text{ Nm}^{-1}$). The relationship between flow rate, pore size, and po number can be expressed by Hagen–Poiseuille Eq. (4) (Shi et al. 2012):

$$Q = \frac{n\pi r^4 P}{8\eta L} \quad (4)$$

where Q is the flow rate of the liquid (m^3/s); η is the viscosity of displacement phase, (Pas); L is the thickness of the membrane (m); n is the number of membrane pores.

The mechanical properties of PVDF membranes were mainly investigated in terms of tensile strength and elongation at break. At first, the thickness of the flat sheet membrane was measured (by thickness gauge) and recorded. Then, a rectangle shape of membrane with a length of 5 cm and a width of 0.5 cm was taken as a sample and tested by a tensile stress–strain meter (SH-20, SUND00, China). The initial length of the sample is recorded as L_0 , and the sample is drawn slowly at a constant speed until it breaks. The length of the membrane L and the tensile force F shown by the tensimeter are recorded respectively when the membrane was broke. The test was repeated five times for the membrane prepared under the same condition. The formulas for calculating the tensile strength and elongation at break are as follows:

$$\sigma = \frac{F}{A} \quad (5)$$

$$\varepsilon = \frac{L - L_0}{L_0} \times 100\% \quad (6)$$

where σ stands for tensile stress (MPa), and ε stands for elongation at break (%). A is the cross-sectional area of the membrane (m^2).

Results and discussion

Phase diagram

Preparation PVDF membrane by TIPS is a kind of non-equilibrium process, so the effect of cooling speed on the phase diagram should be considered. The phase diagram of PVDF/[BMIM]BF₄ system is shown in Fig. 2. It shows that with the increase of polymer content, the crystallization temperature of the casting solution also increases gradually. This is mainly because the compatibility of PVDF/[BMIM]BF₄ binary system decreases gradually with the increase of PVDF concentration (Jung et al. 2016). When the polymer concentration is within the range of 10 wt% to 50 wt%, the cloud point curve is always above the crystallization curve. Within the range of 10–40 wt%, the cloud point increases with the increase of polymer concentration; while the polymer concentration is higher than 40 wt%, and the cloud point temperature begins to decrease. Generally speaking, for traditional diluents, the cloud point temperature generally decreases with the increase of polymer concentration, and the cloud point curve intersects with the crystallization curve (called the monotectic point). Also, when the concentration of polymer is lower than the monotectic point, the L-L phase separation occurs in the casting liquid system during the cooling process, and the microstructure of the membrane presents a bi-continuous structure. When the concentration of polymer is higher than the monotectic point, the S-L phase separation occurs, and the microstructure of the membrane presents a spherulite structure (Cui et al. 2018b). In this paper, the phase diagram of PVDF/[BMIM]BF₄ system has no monotectic point in the range of 10–50 wt%, and this system has a wide L-L phase separation region. In principle, when the polymer concentration is within the range of

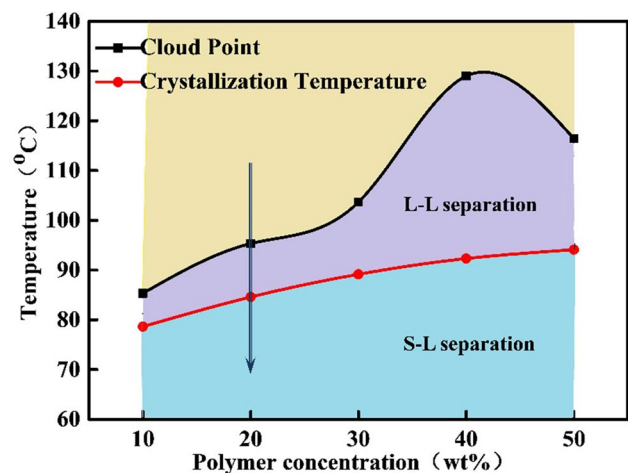


Fig. 2 Phase diagram of PVDF/[BMIM]BF₄ system

10–50 wt%, L-L phase separation will take place preferentially as the temperature of casting solution decreases, and S-L phase separation will dominate when the temperature is further lower than the crystallization temperature. When the polymer concentration is 20 wt%, the cooling path of the casting solution is shown by the arrow in Fig. 2. When the homogeneous casting solution with high temperature cooling to the cloud point, it enters a narrow L-L phase separation region. As the temperature continues to drop below the crystallization temperature, the system enters the S-L phase separation region.

Effect of quenching temperature

Morphology

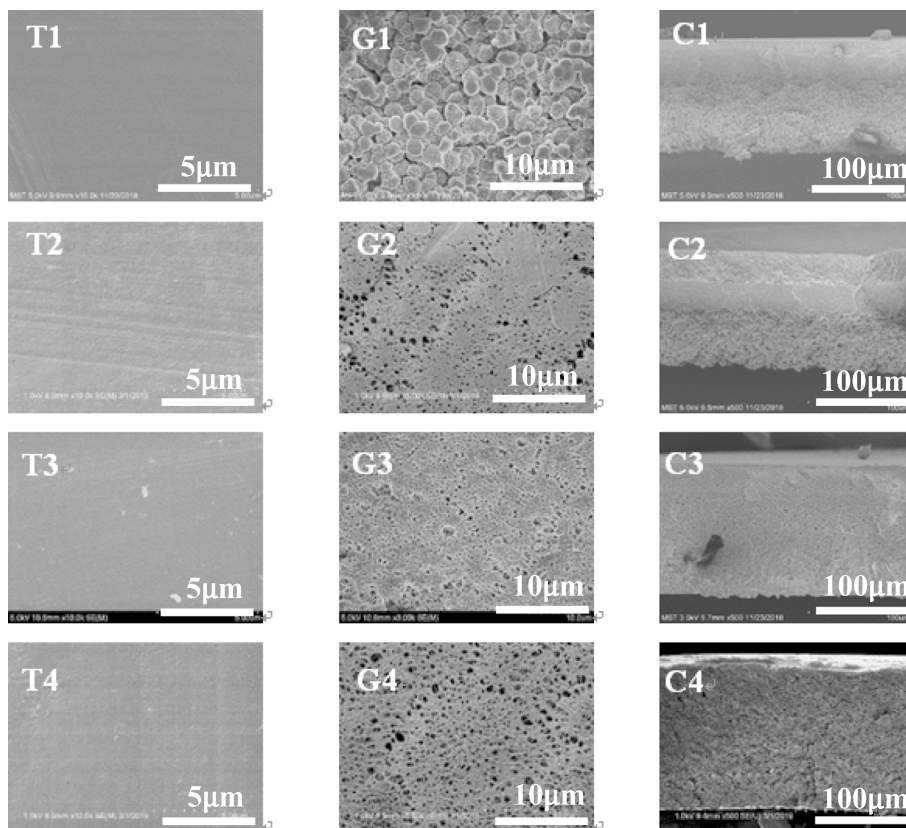
The SEM images of the membranes prepared at different quenching temperatures are shown in Fig. 3. It shows the morphologies of the top surface (T1–T4), the glass side (G1–G4, under surface) and the cross section (C1–C4) of the membrane, respectively. As shown in Fig. 3 T1–T4, all the top surfaces are dense structures. This is because the top surface is affected by the fast phase inversion phenomena.

When the quenching temperature is 15 °C (G1), the under surface of the membrane exhibits a spherulite structure. When the quenching temperature reaches 45 °C (G3),

the under surface becomes a bi-continuous structure. This can be explained by the phase diagram. Under the condition of the experimental concentration, when the quenching temperature is low, the casting solution is cooled rapidly, passing through the L-L phase separation region and entering the S-L phase separation region. This means that, when the quenching temperature is low, the separation time of L-L phase is too short, so S-L phase separation dominates and the spherulite structure is formed. When the quenching temperature is high, the temperature of the casting solution will stay longer time in the L-L phase separation region, which provides enough time for the L-L phase separation, thus forming a bi-continuous structure.

From the C1 and C2 in Fig. 3, it can be seen that besides the spherulite structure, the cross sections of M1 and M2 also have dense layer, which is due to the formation of gel layer. This is attributable to the appearance of PVDF nuclei in PVDF/[BMIM]BF₄ mixtures. As the nuclei generate and grow up, the polymer network gradually comes into being, and significant chain entanglement, bringing big torsion force hinders the spindle rotation. It was illustrated by the fact that sol–gel transition of PVDF/[BMIM]BF₄ solutions is also occurred by crystallization-induced gelation mechanism (Tazaki et al. 1997). In addition, M1 has more spherulites structure than that of M2, lower quenching temperature is conducive to S-L phase separation and promotes

Fig. 3 SEM images of PVDF membranes prepared at different quenching temperatures



the formation of spherulite structure. The cross section of M3 (C3) shows a completely sponge-like structure, which indicates that the sol–gel transition can be avoided at high quenching temperature. Therefore, high quenching temperature is selected for further investigation of introduced IL (Table 2).

Porosity, water permeability and mechanical properties

The flux, porosity, tensile strength and elongation at break of the membranes at different quenching temperatures are listed in Table 3. The porosity of the membranes increased with the increase of quenching temperature. When the quenching temperature is low, the phase separation is dominated by S-L phase separation, resulting in the formation of a thick dense layer. Therefore, the porosity of the film at 15 °C and 30 °C is very low, which is 52.7% and 57.9%, respectively. When the quenching temperature increased, the phase separation was dominated by the L-L phase separation, forming a bi-continuous structure, and the pore connectivity was improved, so the porosity increased significantly. When the quenching temperature was 60 °C, the porosity increased to 77.4%. It can be seen from Table 3 that with the increase of quenching temperature, the flux of the membranes increases, which is consistent with the porosity and the microstructure of the membranes presented by SEM. When the quenching temperature was increased to 45 °C, the flux was nearly twice as high as that at 30 °C. This is mainly because the membranes formed at high quenching temperature has a thin skin layer.

Table 2 Dope compositions used for membrane preparation

Code	PVDF(wt%)	[BMIM] BF4(wt%)	PVP(wt%)	Quenching temperature(°C)
M1	20	80	0	15
M2	20	80	0	30
M3	20	80	0	45
M4	20	80	0	60
M5	20	79	1	45
M6	20	77	3	45
M7	20	75	5	45
M8	20	70	10	45

Table 3 Porosity, water permeability, tensile stress and elongation of PVDF membranes produced with different quenching temperatures

Quenching temperature(°C)	Porosity(%)	Water permeability(L/m ² h)	Tensile stress(MPa)	Elongation(%)
15(M1)	52.67 ± 2.31	16.88 ± 0.72	1.91 ± 0.09	10.12 ± 0.43
30(M2)	57.90 ± 2.57	17.04 ± 0.63	2.03 ± 0.11	9.82 ± 0.38
45(M3)	71.50 ± 3.28	46.20 ± 1.85	4.85 ± 0.20	59.80 ± 3.03
60(M4)	77.42 ± 3.39	60.60 ± 2.01	7.43 ± 0.29	134.9 ± 4.19

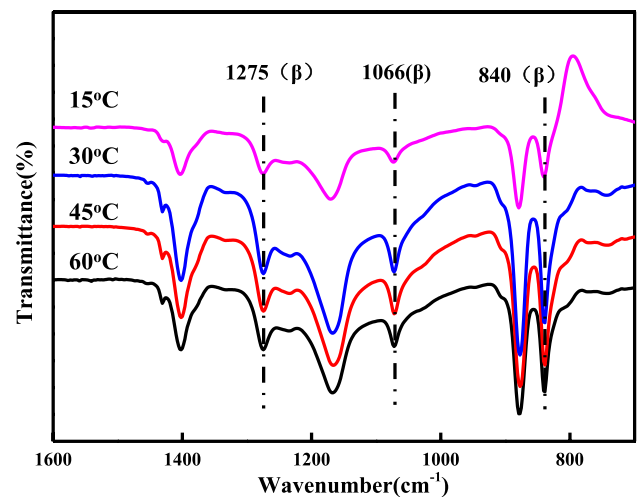


Fig. 4 FTIR spectra of PVDF membranes produced with different quenching temperatures

The tensile strength and elongation at break of the film increased with the increase of quenching temperature. Compared with the membranes at 15 °C and 30 °C, the strength of the membranes at 45 °C was more than doubled. This is because the bi-continuous structure obtained by L-L phase separation in the upper layer section has higher tensile strength than the spherulite structure obtained by S-L phase separation. The tight winding between PVDF molecules can improve the strength and elongation at break of the membranes. The strength and elongation at break of PVDF membranes prepared at 60 °C quenching temperature reached 7.43 MPa and 134.9%, which was mainly attributed to the decrease and disappearance of dense layer due to higher quenching temperature. The dense layer would reduce the toughness of the membranes, and the reduction of dense layer would help improve the mechanical properties of the membrane.

Crystals of PVDF membranes

The FTIR spectra of the flat sheet membranes prepared under different quenching temperature are presented and compared in Fig. 4, in which the transmittance (%) is a function of wavelength (cm⁻¹).

Generally, the IR absorption bands at approximately 1211, 1149, 1069, 975, 854, 794, and 763 cm^{-1} represent the characteristic spectrum of an α phase PVDF crystal; whereas the absorption bands at 511, 600, 840, 1066, and 1275 cm^{-1} represent the characteristic spectrum of β phase PVDF (Cui et al. 2015b). The 1288 cm^{-1} and 840 cm^{-1} bands were assigned to symmetric CF_2 stretching vibrations of β -phase sequences comprising three or more sequential transmonomeric units. It can be seen from FTIR images that there are obvious characteristic peaks at 840, 1066 and 1275 cm^{-1} , and there is no corresponding characteristic peak of α , which indicates that the prepared PVDF membrane is pure β phase, and the change of quenching temperature will not affect the crystal form of the membrane. This is due to the strong electrostatic effect of ionic liquids on the formation of higher energy β crystals in PVDF.

In order to further obtain information related to the polymorphisms of PVDF membranes in this study, WAXD (wide angle X-ray diffraction) measurements were performed and the diffraction patterns of PVDF membranes produced at different quenching temperatures are presented in Fig. 5. The characteristic diffraction peaks of the α phase are 17.4°, 18.1°, 19.6°, 26.5°, corresponding to 100, 020, 110, 021 crystal plane, respectively. 20.26° is for the β phase 110 and 200 lattice plane; 18.4°, 20.2°, and 26.6° are for the γ phase 020, 002, 110 crystal plane, respectively (Cui et al. 2015b). It can be seen from the figure that the PVDF membranes prepared at all temperatures have diffraction peaks only at 20.26°, which further shows that the PVDF membranes prepared by using [BMIM]BF₄ as diluent are a pure β phase.

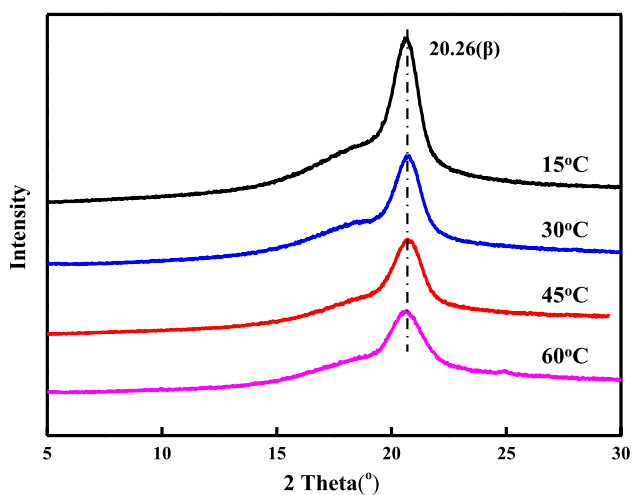


Fig. 5 XRD results of PVDF membranes produced with different quenching temperatures

Effect of additive content

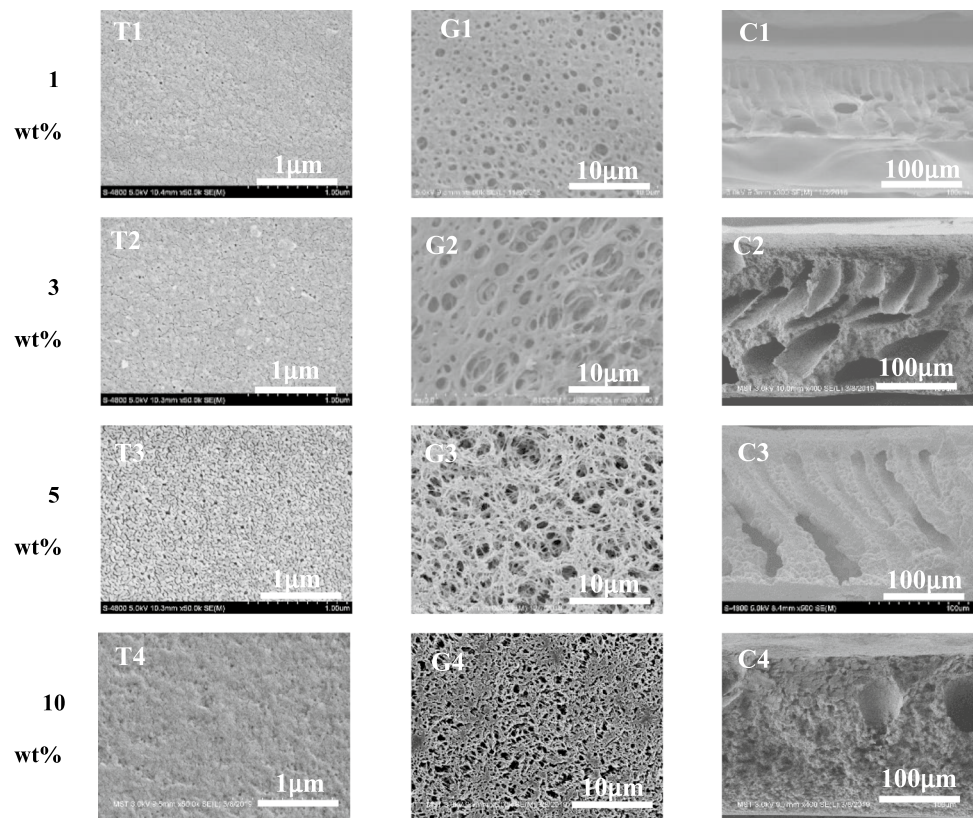
Due to the water solubility of IL, PVDF membranes prepared by PVDF/IL system undergo both TIPs and NIPs and it would produce a dense layer, which leads to low permeability. Polyvinylpyrrolidone is usually utilized as porogen and hydrophilic modification additive for PVDF membranes. PVP with different molecular weight and content can effectively improve the porosity and hydrophilicity of PVDF membranes. Therefore, the effect of different concentration of PVP on PVDF membrane was studied.

The morphology of the membranes with different PVP concentrations is shown in Fig. 6. It can be seen from T1-T4 in Fig. 6 that PVP plays the role of opening the membrane pores. As a pore-forming agent, PVP can effectively improve the porosity of the membrane surface at low concentration. At high concentrations, PVP molecules have a high degree of binding with PVDF long chain, which cannot be completely removed in the post-treatment of the membrane. The more PVP is added, the more residual in the membrane, thus increasing the total polymer content of the membrane. Therefore, when the concentration of PVP reaches 10 wt %, the porosity of the membrane surface decreases.

After adding PVP, the morphology of the bottom of the membrane showed sponge-like structure, indicating that L-L phase separation occurred near the glass side. On the one hand, as mentioned above, high quenching temperature is conducive to promoting L-L phase separation. On the other hand, the addition of PVP can delay the crystallization of the casting solution system. The addition of PVP can reduce the crystallization temperature of the casting solution significantly, and the crystallization temperature decreases with the increase of the content of PVP. This means that there is a larger L-L phase separation region, which is more conducive to the occurrence of L-L phase separation, so the bottom of the membrane formed a sponge-like structure.

The cross sections (C1–C4) of the membranes showed asymmetrical structures with layer and finger-like holes. With the increase of PVP concentration, the proportion of support layer increases, and the finger-shaped hole tends to decrease. When the concentration reaches 10wt %, the finger-like hole decreases obviously. At low PVP concentration, the viscosity of the casting solution is low, and the solvent–non-solvent diffusion is easy. Due to the hydrophilic property of PVP, the diffusion is more promoted, so a large finger-like hole is formed. With the increase of PVP concentration, the viscosity of the casting solution increases, which has an inhibitory effect on solvent–non-solvent diffusion. Therefore, when the concentration of PVP reaches 10wt %, the finger-like hole decreases obviously, which is conducive to improving the mechanical strength of the membrane.

Fig. 6 SEM images of PVDF membranes prepared with different PVP concentrations (T, G, C represent top surface, glass side and cross section, respectively)



Porosity, pure water flux and mechanical properties

When the quenching temperature was 45 °C, the pure water flux, porosity, tensile strength and elongation at break of membranes prepared with different PVP concentrations are listed in Table 4.

The porosity of the membrane first increased and then decreased with the increase of PVP content. This trend is consistent with the situation reflected by the SEM of membrane cross section and surface. Low concentration of PVP is helpful to improve the porosity and pore connectivity, so as to improve the overall porosity of the membrane. When the concentration of PVP is 5 wt%, the maximum porosity reaches 75.8%. However, the high concentration of PVP increased the total polymer content of the membrane and decreased the porosity of the membrane.

The addition of PVP improved the permeability of the membrane significantly. When PVP concentration was

increased to 5 wt%, the membrane flux increased to 383.2 L/m²h. This was attributed to the increase in the number of surface pore on the PVDF membrane. Secondly, the hydrophilic PVP additive improved the hydrophilicity of PVDF membrane, making it easier for water to enter the membrane pores. When the PVP content was 10 wt%, the pure water flux decreased, which was mainly attributed to the decrease of membrane porosity caused by the increase of the total polymer amount.

Compared with M3, the tensile strength of membranes with PVP was lower. Because when PVP is added into PVDF/[BMIM]BF₄ system, it promotes the diffusion between the solvent in the casting solution and the quenching water bath, forming large finger-like holes, which significantly reduces the tensile strength and elongation at break of membrane.

Table 4 Water permeability, porosity, tensile stress and elongation of PVDF membranes produced with different quenching temperatures

PVP concentration (wt%)	Porosity (%)	Water permeability (L/m ² h)	Tensile stress(MPa)	Elongation(%)
1(M5)	72.54 ± 3.63	80.0 ± 2.48	2.84 ± 0.08	30.1 ± 1.51
3(M6)	74.38 ± 5.03	340.4 ± 10.2	2.86 ± 0.08	32.7 ± 1.60
5(M7)	76.80 ± 3.84	383.2 ± 15.33	2.97 ± 0.10	34.3 ± 1.44
10(M8)	74.43 ± 4.01	273.1 ± 13.66	3.53 ± 0.16	30.6 ± 1.53

Pore size distribution

The pore size distribution of PVDF membranes prepared with different PVP concentrations is shown in Fig. 7, and the concentration of pore size and proportion is shown in Table 5. It can be seen from Fig. 7 that the prepared PVDF membranes all have a rather concentrated pore size distribution and the proportion of concentrated pore diameter ranges between 75 and 88%. The variation trend of the concentrated pore diameter was consistent with the SEM (TI–T4) of the membranes in Fig. 6. The concentration of the concentrated pore diameter increased first and then decreased with the increase of PVP concentration. When the concentration of PVP increased from 1 to 5 wt%, the concentrated pore diameter increased from 15 to 26 nm, and when the content of PVP increased to 10 wt%, the concentrated pore diameter decreased to 22 nm.

Hydrophilicity of PVDF membranes

The contact angles of PVDF films prepared with different PVP concentrations are shown in Fig. 8. In the preparation of the PVDF membrane, polyvinylpyrrolidone plays the role of pore-forming agent. Because the molecular structure of PVP contains hydrophilic amide group, it also acts as a hydrophilic modifier. Although PVP is water-soluble, it will be coated by PVDF molecules when membrane formed, which has a high binding degree with PVDF long chain and is difficult to be completely removed in the post-treatment process. Some PVP remains in the membrane bulk and on the surface of the membrane. Therefore, the addition of PVP gradually reduces the contact angle of the membrane from 87.7° to 65.3°, which effectively improves the hydrophilic property of the PVDF membrane. The

Table 5 Pore size distribution of PVDF membranes with different PVP concentrations

PVP concentration(wt%)	Concentrated pore size(nm)	Concentrated pore ratio(%)
1(M5)	15	80
3(M6)	20	86
5(M7)	26	75
10(M8)	22	88

improvement of hydrophilic property is conducive to improving the anti-pollution performance of the membrane and improving the service life of the membrane (Li et al. 2010; Rana and Matsuura 2010).

Phases of PVDF membranes

ATR-FTIR images (Fig. 9) of PVPF membranes prepared at different PVP contents show that the characteristic peaks occur at 840, 1066 and 1275, which are corresponding to the characteristic peaks of β phase in literature(Cui et al. 2015b). No characteristic peaks of the α phase are found, which indicates that the addition of PVP does not affect the formation of β phase induced by ionic liquids. In addition, there was a characteristic peak at 1660, and the peak area increased with the increase of PVP content. This peak is the C=O double bond stretching vibration peak, and this proved that PVP remained in the membrane. Also, the XRD spectra of PVPF membranes prepared at different PVP contents are shown in Fig. 10. The only β peak at 20.26° is also shown in the figure. It is further proved that the PVDF membranes with different PVP contents are a pure β phase polymorphism.

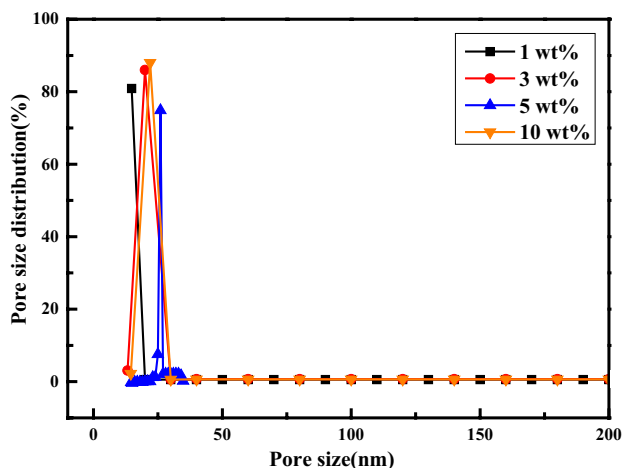


Fig.7 Pore size distribution of PVDF flat sheet membrane with different PVP content

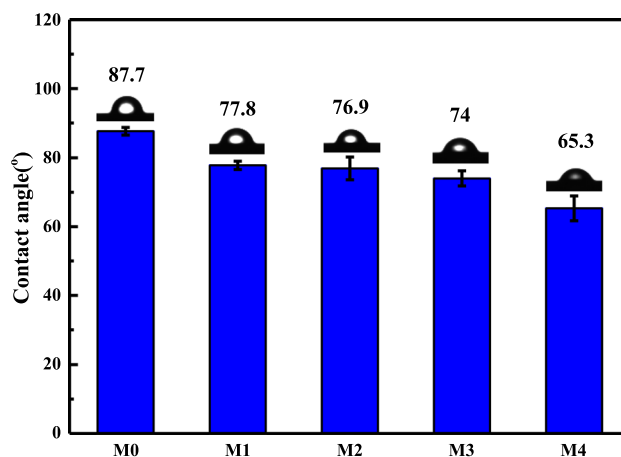


Fig.8 Contact angle of PVDF flat sheet membrane with different PVP content

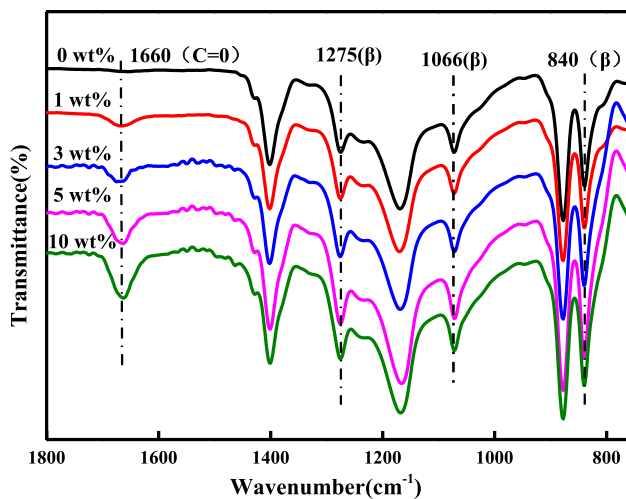


Fig. 9 FTIR spectra of PVDF membranes produced with different PVP concentrations

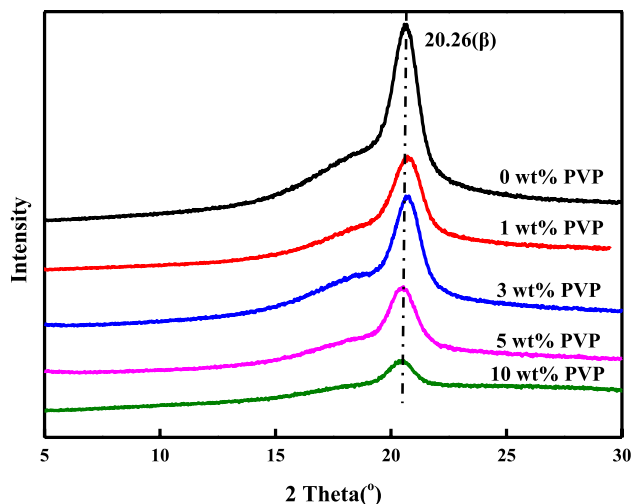


Fig. 10 XRD results of PVDF membranes produced with different PVP concentrations

Conclusions

In this study, pure β -phase PVDF membranes with a narrow pore size distribution were successfully prepared by using [BMIM]BF₄ as the single diluent via N-TIPS method. The effect of quenching temperature and PVP concentration on the micro-structure and properties of the PVDF flat membranes were discussed. A sponge-like structure is obtained at a high quenching temperature, and a narrow pore size distribution with concentrated pore size around 20 nm is formed at a certain PVP concentration.

The antifouling properties was promising due to the β phase and the hydrophilicity of the membranes.

Acknowledgements The chinese authors would like to express their appreciation for the National Natural Science Foundation of China (22078146), the financial support of the National Key R&D Program of China (2020YFC0862703), the Natural Science Foundation of Jiangsu Province (BK20200091), Six Talent Peaks Project in Jiangsu Province (JNHB-036), the Materials-Oriented Chemical Engineering State Key Laboratory Program (KL19-04). Naser Tavajohi appreciate the financial support from Kempe Foundation (SMK-1850).

Funding The National Natural Science Foundation of China (22078146), the financial support of the National Key R&D Program of China (2020YFC0860903), the Natural Science Foundation of Jiangsu Province (BK20200091), Six Talent Peaks Project in Jiangsu Province (JNHB-036), the Materials-Oriented Chemical Engineering State Key Laboratory Program (KL19-04), Kempe Foundation (SMK-1850).

Declarations

Conflict of interest The author declares that there is no conflict of interest.

Open Access This article is licensed under a Creative Commons Attribution 4.0 International License, which permits use, sharing, adaptation, distribution and reproduction in any medium or format, as long as you give appropriate credit to the original author(s) and the source, provide a link to the Creative Commons licence, and indicate if changes were made. The images or other third party material in this article are included in the article's Creative Commons licence, unless indicated otherwise in a credit line to the material. If material is not included in the article's Creative Commons licence and your intended use is not permitted by statutory regulation or exceeds the permitted use, you will need to obtain permission directly from the copyright holder. To view a copy of this licence, visit <http://creativecommons.org/licenses/by/4.0/>.

References

- Coster HGL, Farahani TD, Chilcott TC (2011) Production and characterization of piezo-electric membranes. *Desalination* 283:52–57
- Cui Z, Hassankiadeh NT, Lee SY, Lee JM, Woo KT, Sanguineti A, Arcella V, Lee YM, Drioli E (2013) Poly(vinylidene fluoride) membrane preparation with an environmental diluent via thermally induced phase separation. *J Membr Sci* 444:223–236
- Cui Z, Hassankiadeh NT, Lee SY, Woo KT, Lee JM, Sanguineti A, Arcella V, Lee YM, Drioli E (2015a) Tailoring novel fibrillar morphologies in poly(vinylidene fluoride) membranes using a low toxic triethylene glycol diacetate (TEGDA) diluent. *J Membr Sci* 473:128–136
- Cui ZL, Hassankiadeh NT, Zhuang YB, Drioli E, Lee YM (2015b) Crystalline polymorphism in poly(vinylidene fluoride) membranes. *Prog Polym Sci* 51:94–126
- Cui ZL, Cheng YM, Xu K, Yue J, Zhou Y, Li XG, Wang Q, Sun SP, Wang Y, Wang XZ, Wang ZH (2018b) Wide liquid-liquid phase separation region enhancing tensile strength of poly(vinylidene fluoride) membranes via TIPS method with a new diluent. *Polymer* 141:46–53
- Cui Z, Cheng Y, Xu K, Yue J, Zhou Y, Li X, Wang Q, Sun SP, Wang Y, Wang X, Wang Z (2018a) Wide liquid-liquid phase separation region enhancing tensile strength of poly(vinylidene fluoride)

- membranes via TIPS method with a new diluent, *Polymer: The International Journal for the Science and Technology of Polymers* Deka M, Kumar A (2011) Electrical and electrochemical studies of poly(vinylidene fluoride)-clay nanocomposite gel polymer electrolytes for Li-ion batteries. *J Power Sources* 196:1358–1364
- Garcia-Ivars J, Alcaina-Miranda M-I, Iborra-Clar M-I, Mendoza-Roca J-A, Pastor-Alcañiz L (2014) Enhancement in hydrophilicity of different polymer phase-inversion ultrafiltration membranes by introducing PEG/Al₂O₃ nanoparticles. *Sep Purif Technol* 128:45–57
- Hassankiadeh NT, Cui Z, Kim JH, Shin DW, Lee SY, Sanguineti A, Arcella V, Lee YM, Drioli E (2015) Microporous poly(vinylidene fluoride) hollow fiber membranes fabricated with PolarClean as water-soluble green diluent and additives. *J Membr Sci* 479:204–212
- Imai Y, Kimura Y, Niwano M (2012) Organic hydrogen gas sensor with palladium-coated beta-phase poly(vinylidene fluoride) thin films. *Appl Phys Lett* 101:181907
- Jung JT, Kim JF, Wang HH, Nicolo ED, Drioli E, Lee YM (2016) Understanding the non-solvent induced phase separation (NIPS) effect during the fabrication of microporous PVDF membranes via thermally induced phase separation (TIPS). *J Membr Sci* 514:250–263
- Kepler RG, Anderson RA (1978) Piezoelectricity and pyroelectricity in polyvinylidene fluoride. *J Appl Phys* 49:4490–4494
- Kim D, Moreno N, Nunes SP (2016) Fabrication of polyacrylonitrile hollow fiber membranes from ionic liquid solutions. *Polym Chem* 7:113–124
- Lee CS, Joo J, Han S, Lee JH, Koh SK (2004) Actuation of PVDF cantilever with PEDOT/PSS (DIVISO) electrode using ion-assisted-reaction. *J Korean Phys Soc* 45:747–750
- Li N, Xiao C, An S, Hu X (2010) Preparation and properties of PVDF/PVA hollow fiber membranes. *Desalination* 250:530–537
- Livazovic S, Li Z, Behzad AR, Peinemann KV, Nunes SP (2015) Cellulose multilayer membranes manufacture with ionic liquid. *J Membr Sci* 490:282–293
- Lovinger AJ (1982) Annealing of poly(vinylidene fluoride) and formation of a fifth phase. *Macromolecules* 15:40–44
- Martins P, Costa CM, Lanceros-Mendez S (2011) Nucleation of electroactive beta-phase poly(vinylidene fluoride) with CoFe₂O₄ and NiFe₂O₄ nanofillers: a new method for the preparation of multiferroic nanocomposites. *Appl Phys A-Mater Sci Process* 103:233–237
- Martins P, Lopes AC, Lanceros-Mendez S (2014) Electroactive phases of poly(vinylidene fluoride): determination, processing and applications. *Prog Polym Sci* 39:683–706
- Ohigashi H, Watanabe T, Li GR, Hattori T, Takahashi S (1991) Piezoelectric properties of β -form PVDF films crystallized at high pressure and their applications to heat-resistant ultrasonic transducers. *Jpn J Appl Phys* 30:111–113
- Rana D, Matsuura T (2010) Surface modifications for antifouling membranes. *Chem Rev* 110:2448–2471
- Ribeiro C, Panadero JA, Sencadas V, Lanceros-Mendez S, Tamano MN, Moratal D, Salmeron-Sanchez M, Gomez Ribelles JL (2012) Fibronectin adsorption and cell response on electroactive poly(vinylidene fluoride) films. *Biomed Mater* 7:035004
- Salimi A, Yousefi AA (2003) FTIR studies of beta-phase crystal formation in stretched PVDF films. *Polym Test* 22:699–704
- Shi F, Ma Y, Ma J, Wang P, Sun W (2012) Preparation and characterization of PVDF/TiO₂ hybrid membranes with different dosage of nano-TiO₂. *J Membr Sci* 389:522–531
- Su YP, Sim LN, Li X, Coster HGL, Chong TH (2021) Anti-fouling piezoelectric PVDF membrane: Effect of morphology on dielectric and piezoelectric properties. *J Membr Sci* 620:118818
- Szekely G, Jimenez-Solomon MF, Marchetti P, Kim JF, Livingston AG (2014) Sustainability assessment of organic solvent nanofiltration: from fabrication to application. *Green Chem* 16:4440–4473
- Tazaki M, Wada R, Okabe M, Homma T (1997) Crystallization and gelation of poly(vinylidene fluoride) in organic solvents
- Wormald P, Ameduri B, Harris RK, Hazendonk P (2006) Fluorine-19 solid state NMR study of vinylidene fluoride polymers using selective relaxation filters. *Solid State Nucl Mag* 30:114–123
- Yue J, Cheng Y (2018) Efficient preparation of piezoelectric pvdf membrane by thermally induced phase separation, *Chinese J Chem Eng*

Publisher's Note Springer Nature remains neutral with regard to jurisdictional claims in published maps and institutional affiliations.